

Manuscript Number: PLAC-S-19-00107R3

Title: TROPHOBLAST-INDUCED SPIRAL ARTERY REMODELLING AND UTEROPLACENTAL HAEMODYNAMICS IN PREGNANT RATS WITH INCREASED BLOOD PRESSURE INDUCED BY HEME OXYGENASE INHIBITION.

Article Type: Original article

Keywords: Trophoblast invasion, placenta, uteroplacental haemodynamics, vascular remodelling, hypertension, Doppler ultrasonography.

Corresponding Author: Dr. María Teresa Llinás, Ph.D.

Corresponding Author's Institution: University of Murcia

First Author: Lidia Oltra

Order of Authors: Lidia Oltra; Virginia Reverte; María Belén Garcés; Giovanni Li Volti; Juan Manuel Moreno; Francisco Javier Salazar; María Teresa Llinás, Ph.D.

Abstract: Objective

The aim of the present study was to determine the contribution of the heme oxygenase (HO) system to the adaptation of the uteroplacental circulation to pregnancy in the rat, and its relationship with the maintenance of blood pressure during late gestation.

Methods

The HO inhibitor, stannous mesoporphyrin (SnMP), or vehicle were administered intraperitoneally to virgin and midpregnant rats. Mean arterial pressure (MAP) was measured before and after the treatment, in the conscious rats. Uterine and radial arteries blood flow velocities were obtained from pregnant rats at days 14 and 19 of gestation using high frequency ultrasonography. Trophoblast invasion and spiral arteries remodelling were analyzed in the mesometrial triangle of pregnant rats by immunohistochemistry.

Results

HO activity inhibition during late gestation induced a significantly increase in the MAP of pregnant rats ( $114 \pm 1$  mmHg vs  $100 \pm 2$  mmHg,  $p < 0.05$ ) but it did not affect this parameter in virgin rats ( $121 \pm 2$  mmHg vs  $124 \pm 3$  mmHg). MAP elevation was associated with marked ( $p < 0.05$ ) decreases in the systolic and diastolic flow velocities in uterine and radial arteries, as compared with pregnant control rats. Furthermore, spiral arteries of pregnant rats treated with SnMP showed lower ( $p < 0.001$ ) proportion of lumen circumference covered by trophoblast ( $21 \pm 3\%$ ) and a higher ( $p < 0.05$ ) proportion of vascular smooth muscle ( $33 \pm 5\%$ ) than control pregnant rats ( $59 \pm 5\%$  and  $16 \pm 5\%$ , respectively)

Conclusions

These data indicate that HO system play an important role in the adaptation of the uteroplacental circulation to pregnancy and in the blood pressure regulation during late gestation.



Response to reviewers.

Reviewer #1:

Trophoblast has been corrected in the abstract.

New pictures have been introduced. We have tried to find pictures illustrating the mean of the values obtained from the immunohistochemistry studies. As we explain in the manuscript, the data shown are the means of all values obtained from the quantification of all spiral arteries from each implantation site, therefore it is difficult that all the pictures, showing these data in the same vessel with the three different immunostaining methods, are good. We have also introduced two new pictures in figure 3 at low augmentation indicating the localization of the vessel.

In regard to show the pictures in the same figure, we have put together in figure 3 all the images. Although it is better to compare both groups, to show pictures in separate figures allows a greater amplification. That was the reason why we shown the images in different figures in the last version of the manuscript .

Reviewer #3:

Thank you for you comments. As the reviewer indicates, our results show that HO is involved in the regulation of blood pressure during late gestation and confirm previous studies which have found significant increases in diastolic blood pressure during pregnancy in HO-1-deficient mice. In our study, pregnant rats treated with the HO inhibitor showed higher levels of mean arterial pressure at late gestation than pregnant rats treated with vehicle ( $114 \pm 1$  mmHg vs  $100 \pm 2$  respectively ), indicating that HO inhibition impaires the decrease in blood pressure associated with pregnancy. Although an increase of 14 mmHg in mean arterial pressure suggests a significative elevation of diastolic blood pressure in our study, we agree with the reviewer that with these levels of pressure we can not speak of hypertension. We have replaced “hypertension” by “increase in blood pressure” in the manuscript and we have introduced a sentence in the discussion explaining it (lines 311-315).

In regard to the RUPP model, George et al have demonstrated that HO-1 induction with cobalt protoporphyrin attenuates hypertension in these animals indicating, as the reviewer suggests, that HO-1 or its metabolites are potential therapeutics for the treatment of pregnancy induced hypertension. This idea has been discussed in the manuscript (lines 357-360).

New pictures have been introduced. I have tried to find pictures illustrating the mean of the values obtained from the immunohistochemistry studies. As we explain in the manuscript, the data shown are the means of all values obtained from the quantification of all spiral arteries from each implantation site, therefore it is difficult that all the pictures, showing these data in the same vessel with the three different immunostaining methods, are good. As the reviewer suggest we have introduced two new pictures at low augmentation indicating the localization of the vessels.

# Author Agreement

## AUTHOR AGREEMENT

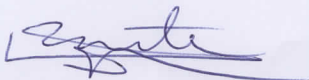
We confirm that the manuscript has been read and approved by all named authors and that there are no other persons who satisfied the criteria for authorship but are not listed. We further confirm that the order of authors listed in the manuscript has been approved by all of us.

Signed by all authors:

Lidia Oltra



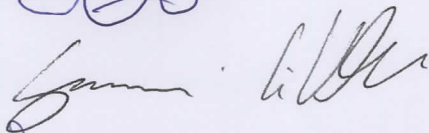
Virginia Reverte



Belen Garcés



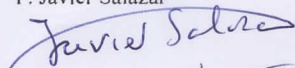
Giovanni Li Volti



J. Moreno



F. Javier Salazar



M. Teresa Llinás



CONFLICT OF INTEREST STATEMENT

We wish to confirm that there are no known conflicts of interest associated with this publication and there has been no significant financial support for this work that could have influenced its outcome.

Signed by all authors:

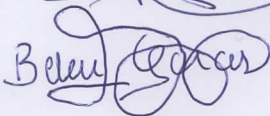
Lidia Oltra



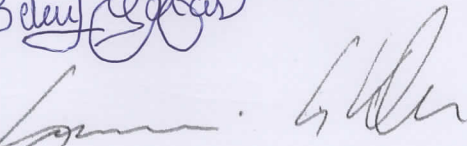
Virginia Reverte



Belen Garcés



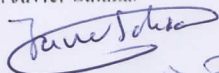
Giovanni Li Volti



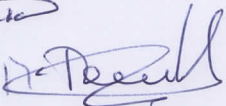
J. Moreno



F. Javier Salazar



M. Teresa Llinás



1 TROPHOBLAST-INDUCED SPIRAL ARTERY REMODELLING AND  
2 UTEROPLACENTAL HAEMODYNAMICS IN PREGNANT RATS WITH  
3 INCREASED BLOOD PRESSURE INDUCED BY HEME OXYGENASE  
4 INHIBITION.

5  
6 <sup>1</sup>Oltra L, <sup>1</sup>Reverte V, <sup>1</sup>Garcés B, <sup>2</sup>Li Volti G, <sup>1</sup>Moreno JM, <sup>1</sup>Salazar FJ and <sup>1</sup>Llinás MT.

7  
8 <sup>1</sup>Department of Physiology, School of Medicine, University of Murcia and Biomedical  
9 Research Institute in Murcia, Spain; <sup>2</sup> Department of Biomedical and Biotechnological  
10 Sciences, University of Catania, Italy.

11  
12  
13  
14  
15  
16  
17  
18  
19  
20  
21  
22  
23  
24  
25  
26  
27  
28  
29  
30  
31  
32  
33  
34 Author for correspondence:

35 María Teresa Llinás

36 Department of Physiology. School of Medicine.

37 University of Murcia, 30100 Murcia, SPAIN.

38 Phone: 34-868-884395

Fax: 34-868-884150

e-mail: mayte@um.es

39  
40 Declarations of interest: none.

51  
52  
53  
54  
55  
56  
57  
58  
59  
60  
61  
62  
63  
64  
65  
66  
67  
68  
69  
70  
71  
72  
73  
74  
75  
76  
77  
78  
79  
80  
81  
82  
83  
84  
85

**ABSTRACT**

**Objective**

The aim of the present study was to determine the contribution of the heme oxygenase (HO) system to the adaptation of the uteroplacental circulation to pregnancy in the rat, and its relationship with the maintenance of blood pressure during late gestation.

**Methods**

The HO inhibitor, stannous mesoporphyrin (SnMP), or vehicle were administered intraperitoneally to virgin and midpregnant rats. Mean arterial pressure (MAP) was measured before and after the treatment, in the conscious rats. Uterine and radial arteries blood flow velocities were obtained from pregnant rats at days 14 and 19 of gestation using high frequency ultrasonography. Trophoblast invasion and spiral arteries remodelling were analyzed in the mesometrial triangle of pregnant rats by immunohistochemistry.

**Results**

HO activity inhibition during late gestation induced a significantly increase in the MAP of pregnant rats ( $114\pm 1$  mmHg vs  $100\pm 2$  mmHg,  $p<0.05$ ) but it did not affect this parameter in virgin rats ( $121\pm 2$  mmHg vs  $124\pm 3$  mmHg). MAP elevation was associated with marked ( $p<0.05$ ) decreases in the systolic and diastolic flow velocities in uterine and radial arteries, as compared with pregnant control rats. Furthermore, spiral arteries of pregnant rats treated with SnMP showed lower ( $p<0.001$ ) proportion of lumen circumference covered by trophoblast ( $21\pm 3\%$ ) and a higher ( $p<0.05$ ) proportion of vascular smooth muscle ( $33\pm 5\%$ ) than control pregnant rats ( $59\pm 5\%$  and  $16\pm 5\%$ , respectively)

**Conclusions**

These data indicate that HO system play an important role in the adaptation of the uteroplacental circulation to pregnancy and in the blood pressure regulation during late gestation.

**Keywords**

Trophoblast invasion, placenta, uteroplacental haemodynamics, vascular remodelling, hypertension, Doppler ultrasonography.

## HIGHLIGHTS

- Heme oxygenase activity inhibition during pregnancy induces hypertension.
- Uteroplacental haemodynamics is altered by reductions in heme oxygenase activity.
- Heme oxygenase activity inhibition induces defective spiral arteries remodelling.

1  
2  
3  
4  
5  
6

## INTRODUCTION

7 Cardiovascular adaptation to gestation involves complex hemodynamic changes,  
8 including significant increases in cardiac output and blood volume, a marked reduction  
9 in the systemic resistance and a subsequent decline in blood pressure. Uteroplacental  
10 vasculature undergoes significant structural and functional modifications to ensure an  
11 adequate blood supply to the developing placenta and the fetus. In early stages of  
12 pregnancy, trophoblasts invade the uterine spiral arteries, replacing muscular and  
13 endothelial cells of the arterial wall and transforming them in low resistance vessels  
14 with an increased blood flow and reduced pressure (1). Furthermore, uterine, arcuate  
15 and radial arteries show a progressive dilation through gestation, thereby also  
16 contributing to the reduced resistance and the increased blood flow in the uteroplacental  
17 vascular bed (2, 3). Despite the intensive research linking uteroplacental blood flow  
18 alterations with several pregnancy diseases, such as hypertension, preeclampsia,  
19 intrauterine growth restriction and early pregnancy loss (4), the mechanisms leading to  
20 impaired adaptation of uteroplacental circulation in these disorders are still poorly  
21 understood.

22         Recent studies have reported that heme oxygenase (HO) system is an important  
23 regulator of uteroplacental function (5-8). HO, which catalyzes the conversion of heme  
24 to bilirubin and carbon monoxide (CO), is highly expressed in human, rat and mouse  
25 placenta (5, 9, 10) and its deficiency has been associated with growth restriction,  
26 placental dysfunction and fetal loss (5,6,11,12) . Recently, it has been also reported that  
27 the treatment of late pregnant rats with a HO inhibitor provokes hypertension associated  
28 with a decrease in placental vascular endothelial growth factor (VEGF), suggesting that  
29 the contribution of HO system to the regulation of arterial pressure during gestation may  
30 be mediated by the upregulation of proangiogenic factors (13). However, it is unknown  
31 whether hypertension induced by a decreased HO activity during pregnancy is related  
32 with an impaired trophoblast-induced spiral artery remodelling and/or with alterations  
33 in uteroplacental haemodynamics. Therefore, the aim of the current study was to  
34 investigate the contribution of the HO system to the adaptation of the uteroplacental

35 circulation to pregnancy in the rat, and its relationship with the maintenance of blood  
36 pressure during late gestation.

37

## 38 **MATERIAL AND METHODS**

39

### 40 **Animals**

41

42 All studies were performed in female Sprague Dawley (SD) rats purchased from the  
43 University of Murcia Animal Research Laboratory. The study was approved by the  
44 University Review Committee and experimental protocols were designed according to  
45 the National Institutes of Health Guide for the Care and Use of Laboratory Animals.  
46 Animals were housed in an environmentally controlled facility and were allowed free  
47 access to food and water. Rats (12 weeks of age) destined to become pregnant were  
48 mated overnight. The presence of sperm in vaginal smear on the following morning was  
49 considered as the first day of pregnancy.

50

### 51 **HO-1 and HO-2 expression.**

52

53 Implantation sites (placenta with associated mesometrial triangle) were obtained from  
54 pregnant rats at 8 (n=6), 14 (n=5) and 19 (n=4) days of gestation. Tissues samples were  
55 homogenized in ice-cold 50-mmol/L Tris-HCl buffer, pH 7.4, containing 1% NP-40,  
56 0.25% sodium deoxycholate, 1-mmol/L EDTA, and 10% protease inhibitor cocktail  
57 (Sigma -Aldrich). Homogenates (50 µg) were electrophoresed on a 12% polyacrilamide  
58 gel and then transferred to a polyvinylidene difluoride membrane. Membranes were  
59 incubated for 1 h with a 1:1000 dilution of rabbit anti-rat HO-1 monoclonal or HO-2  
60 polyclonal antibodies (Stressgen Biotechnologies). Afterwards, the membranes were  
61 incubated with horseradish peroxidase- conjugated anti-rabbit Ig G (Amersham) at a  
62 dilution of 1:2000. Chemiluminescence detection was performed with the Amersham  
63 ECL detection kit according to the manufacturer's instructions. Protein expression  
64 changes were quantified by densitometry analysis and presented as the ratio of HO  
65 proteins to  $\beta$ -actin expression in samples run in the same gel.

66

### 67 **Measurement of arterial pressure in conscious rats.**

68

69 To determine the role of HO in regulating arterial pressure during gestation, the effects  
70 of a HO inhibitor, stannous mesoporphyrin (SnMP), on mean arterial pressure (MAP)

71 were compared in virgin and pregnant rats. SnMP (Frontier Scientific) was administered  
72 intraperitoneally at a dose of 50  $\mu\text{mol/kg}$  on day 14 of gestation. A similar dose of  
73 SnMP was used in the study of George et al (13). These authors shown that SnMP  
74 reduced significantly HO activity in the liver and the placenta of pregnant rats, 5 days  
75 after its administration. Studies were conducted in 4 groups of rats: virgin rats treated  
76 with vehicle (50 mmol  $\text{Na}_2\text{CO}_3$ ) (n=10) or SnMP (n=10) and pregnant rats treated with  
77 vehicle (n=10) or SnMP (n=10).

78 On day 17 of pregnancy, rats were anesthetized and instrumented with  
79 indwelling carotid catheters (V/3 tubing, SCI), which were tunnelled under the skin and  
80 exteriorized at the back of the neck. On gestational day 19, conscious rats were placed  
81 in individual restraining cages and the carotid catheter was connected to a pressure  
82 transducer. After a 60 minute stabilization period, MAP was monitored for 40 minutes  
83 using a data acquisition system (PowerLab System). At the end of the experiment,  
84 animals were euthanized and the reproductive tract was removed. The number of  
85 healthy embryos and resorption sites was counted and placental tissues were obtained to  
86 HO activity measurement. Implantation sites, including placenta and mesometrial  
87 triangle, were also obtained from these animals to quantify trophoblast remodelling  
88 using immunohistochemistry.

89

#### 90 **Measurement of HO activity**

91

92 To demonstrate the inhibitory effect of SnMP, HO activity was compared in the  
93 implantation sites (placenta with associated mesometrial triangle) from pregnant control  
94 rats and pregnant rats treated with the HO inhibitor. HO activity was measured by  
95 monitoring the conversion of bilirubin by tissue lysate exposure. To achieve that,  
96 homogenates obtained from the implantation sites at day 19 of gestation were combined  
97 with 2mM glucose-6phosphate, 0.2 U of glucose-6-phosphate dehydrogenase, 0.8 mM  
98 of nicotinamide-adenine dinucleotide phosphate and 20.0  $\mu\text{M}$  hemin, in a total reaction  
99 volume of 1200  $\mu\text{l}$ . After 1 hour of incubation at 37° C, bilirubin was extracted with  
100 chloroform and its concentration was determined spectrophotometrically using the  
101 difference in absorbance at wavelengths from  $\lambda 460$  to  $\lambda 530$  nm with an absorption  
102 coefficient of 40 mM/cm. Activity was expressed as nanograms of bilirubin per  
103 microgram of protein per hour.

104

#### 105 **Immunohistochemistry.**

106

107 From 1 to 3 implantations sites of the pregnant rats from each group, including placenta  
108 and mesometrial triangle, were dissected out and submerged in fixative and left at room  
109 temperature for one day. After fixation, the tissues were dehydrated and embedded in  
110 Paraplast Plust according to standard procedures. Sets of 10 parallel sections were cut  
111 from each implantation site parallel to the mesometrial-fetal axis. Parallel sections from  
112 these sets were stained with the periodic acid Schiff (PAS) method, and immunostained  
113 for keratin (KRT) and alpha smooth muscle actin (ACTA). PAS method was used to  
114 detect fibrinoid deposition inside the arterial wall (14-16). KRT was used to identify  
115 trophoblast cells and was detected by a mouse anti-Pan KRT antibody (clone MNF116,  
116 DAKO) at a dilution of 1:50. ACTA was used to monitored smooth muscle cells and  
117 was detected by a mouse anti-ACTA antibody (clone 1A4, DAKO) at a dilution of  
118 1:100. Both antibodies were detected with a peroxidase conjugated goat anti-mouse IgG  
119 (Sigma-Aldrich) followed by diaminobenzidine tetrahydrochloride (DAB; Sigma-  
120 Aldrich) according to standard procedures. Normal rat serum (10% Sigma-Aldrich) was  
121 added during the secondary antibody incubation to decrease non-specific reactions.

122

### 123 **Quantitative analysis of spiral artery histology**

124

125 All stained sections were scanned a 40X with a microscope slide scanner (SCN400F  
126 Leika) and visualized with a digital software (Image Hub, Leika) at 10X magnification.  
127 The number of total, invaded and non-invaded spiral artery sections, were counted in  
128 the whole mesometrial triangle. Additionally, all invaded spiral artery from each stained  
129 section and the same number of non-invaded were copied out in individual parallel  
130 windows and evaluated by trophoblast invasion and spiral artery remodelling with an  
131 image processing program (Image J). Arterioles with a lumen contour less than 150  $\mu\text{m}$   
132 were excluded from this study. Total length of the each spiral artery contour and the  
133 proportion of the lumen circumference covered by endovascular trophoblast, vascular  
134 smooth muscle and fibrinoid were measured. The presence of endovascular trophoblast,  
135 vascular smooth muscle and fibrinoid were expressed as % of the spiral artery contour  
136 length.

137

### 138 **Ultrasonography studies.**

139

140 Uterine and radial arteries blood flow velocities were obtained from pregnant  
141 rats at days 14 and 19 of gestation, before and after treatment with vehicle (n=7) or  
142 SnMP (n=7). Ultrasound scanning was performed using a high-resolution micro-  
143 ultrasound system (Vevo® 3100, VisualSonics, Toronto, Canadá). This has a range of  
144 single-element and high-frequency transducers with different frequencies and focal  
145 depths. MX250 (axial resolution: 50  $\mu$ m; frequency: 25 MHz) and MX400 (axial  
146 resolution: 75  $\mu$ m; frequency: 40 MHz) transducers were used to examine uterine  
147 hemodynamics. The selected transducer was mounted on the Visualsonics integrated  
148 rail system incorporating a micromanipulator for precision adjustment of the probe  
149 position and orientation. Later, B-mode was activated to locate and visualize the  
150 arteries. Imaging depth was set to at 3 to 10 mm and frame-rate was 20 to 30 frames/s.  
151 Blood flow evaluation was carried out by Doppler mode. The frequency of emission  
152 was 21 to 24 MHz in MX250 probe and 30 MHz in MX400 probe. Pulse-repetition  
153 frequency set at 3 to 30 kHz and wall filter was 100 to 250 Hz. Pulsed Doppler gate set  
154 between 0.2 to 0.5 mm and the angle between the Doppler beam and the vessel was <  
155 60°.

156 Rats were anaesthetized with inhaled isoflurane, the hair was removed and a  
157 depilatory cream was applied to increase ultrasound penetration. Animals were placed  
158 in a supine position on a heated imaging platform with integrated temperature sensor  
159 and ECG electrodes. Heart rate, respiratory rate and rectal temperature (36.5-37.5 °C)  
160 were monitored throughout the experiment. A warmed gel was used as an ultrasound  
161 coupling medium. Doppler waveforms were obtained from the uterine artery near the  
162 uterocervical junction, close to the ileac artery and behind the urinary bladder. For  
163 locate uterine artery, the 40 MHz ultrasound probe was positioned in the diagonal plane,  
164 over one centimeter up vaginal vent using the rail system. B-mode was activated to  
165 locate and visualize the urinary bladder. Doppler waveforms from radial arteries were  
166 obtained using the 40 MHz probe during the second week of pregnancy and the 25 MHz  
167 probe during the third week. Ultrasound evaluation was performed in four embryos in  
168 each rat, two in the left horn and two in the right horn. The probe was placed in  
169 transversal position under thorax, at first on the right side and later, on the left side.  
170 With the rail system, probe was moving from top to down to localize each embryo and  
171 acquire the image.

172 Doppler flow velocity waveforms were obtained in the uterine and radial arteries  
173 from both experimental groups of pregnant rats on day 19 of gestation. The highest

174 point of the systolic waveform was considered as the peak systolic velocity (PSV) and  
175 the point of the diastolic waveform was considered as the end diastolic velocity (EDV).  
176 Both PSV and EDV were measured from at least five consecutive cardiac cycles. Mean  
177 velocity (Vm) and velocity time integral (VTI) were measured by outlining five  
178 consecutive heartbeat cycles. Ultrasound was performed by the same trained operator.  
179 Data were transferred to an ultrasound image workstation for subsequent analysis (Vevo  
180 LAB 3.0.0).

181

### 182 **Statistical analysis.**

183

184 GB-STAT version 6.5 was used for statistical analysis. All data are presented as means  
185  $\pm$  SE. The results were subjected to analysis of variance (ANOVA) for repeated  
186 measures and Fisher's test. A level of  $p < 0.05$  was considered significant.

187

## 188 **RESULTS**

189

### 190 **HO-1 and HO-2 expression.**

191

192 A representative western blot of HO-1 and HO-2 expression at the implantation  
193 site during pregnancy is shown in figure 1A. Densitometry analysis (figure 1B) revealed  
194 that both isoforms are expressed at implantation sites throughout gestation. HO-1 and  
195 HO-2 levels peaked on day 14 of gestation, being significantly higher than the levels  
196 observed on day 8 of pregnancy. Additionally, both isoforms declined slightly at late  
197 gestation.

198

### 199 **Arterial pressure in conscious rats.**

200

201 As can be seen in figure 2A, pregnant control rats, on day 19 of gestation,  
202 showed levels of MAP significantly lower than virgin control rats ( $100 \pm 2$  mmHg vs.  
203  $121 \pm 2$  mmHg, respectively). The inhibition of HO activity with SnMP induced an  
204 increase ( $p < 0.05$ ) in MAP in pregnant rats ( $114 \pm 1$  mmHg) but not in virgin rats ( $124 \pm$   
205  $3$  mmHg). Furthermore, blood pressure elevation in pregnant rats was associated with a  
206 significant reduction in placental HO activity at 19 day of gestation ( $10.4 \pm 0.5$  vs.  
207  $6.9 \pm 0.2$  ng/bilirubin/ $\mu$ g protein/h) (figure 2B), demonstrating that 5 days after  
208 administration, the dose of SnMP used in our study had a significant inhibitory effect on

209 HO activity. Pregnant rats with an increased blood pressure at late gestation had also  
210 higher ( $p<0.05$ ) fetal resorption rate (19%) than control rats (5%).

211

### 212 **Endovascular trophoblast and associated remodelling in the whole mesometrial** 213 **triangle.**

214

215 A total of 13 and 12 implantation sites from 6 pregnant control rats and 7  
216 pregnant rats treated with the HO inhibitor, respectively, were examined. Figure 3  
217 shows trophoblast invasion in the mesometrial triangle from a pregnant control rat (3A)  
218 and a pregnant rat treated with the HO inhibitor (3B). This figure also shows parallel  
219 cross-sections of spiral arteries immunostained for KRT, PAS and ACTA from a control  
220 rat (3C,3E,3G, respectively) and from a pregnant treated rat (3D,3F,3H, respectively).

221 As previously described (14), endovascular trophoblast into the mesometrial triangle  
222 spiral arteries did not form a continuous covering of the whole circumference of the  
223 vessel (figure 3C, 3D) and fibrinoid material was observed underneath the luminal  
224 trophoblast layer (figure 3G, 3H). We also observed fragmentation of the vascular  
225 smooth muscle in invaded vessels (figure 3E, 3F). On day 19 of gestation, the  
226 percentage of spiral arteries invaded by trophoblast was similar in both groups (19% vs.  
227 18%, respectively). However, the proportion of lumen circumference covered by  
228 endovascular trophoblast in the arterial cross sections was significantly ( $p<0.001$ ) lower  
229 in pregnant rats treated with the HO inhibitor ( $21\pm3\%$ ) than in control pregnant rats  
230 ( $59\pm5\%$ ). The amount of fibrinoid in the spiral arteries, expressed as a percentage of  
231 the lumen contour, showed a similar pattern, with lower ( $p<0.05$ ) fibrinoid deposition  
232 ( $22\pm3\%$ ) in pregnant rats with diminished HO activity than in control rats ( $42\pm7\%$ ).  
233 Contrarily, the length of the vascular smooth muscle layer versus the total vessel  
234 contour was significantly higher ( $33\pm5\%$ ) in pregnant rats with a reduction in HO  
235 activity than in pregnant control rats ( $16\pm5\%$ ).

236

### 237 **Uterine and radial arteries blood velocity.**

238

239 Figure 4A shows a representative Doppler flow velocity waveforms obtained in the  
240 uterine and radial arteries from both experimental groups of pregnant rats on day 19 of  
241 gestation. As shown in figure 4B and 4C, PSV and EDV increased significantly from  
242 day 14 to day 19 in uterine and radial arteries of pregnant control rats. However, in the  
243 pregnant rats treated with the HO activity inhibitor, these parameters were similar on

244 days 14 and 19 of gestation. In figure 4A it can be also observed that on day 19 of  
245 gestation, PSV and EDV were lower in uterine and radial arteries of pregnant rats with  
246 reduced HO activity than in control animals. Vm and VTI followed the same pattern  
247 (table 1), showing marked increase on day 19 of gestation in control rats and no changes  
248 in the pregnant rats with diminished HO activity.

249

## 250 **DISCUSSION**

251

252 The main purpose of the present study was to determine the importance of HO  
253 system in regulating the adaptation of uteroplacental circulation and blood pressure to  
254 late gestation in the rat. Our major findings were that reduced HO activity during late  
255 gestation led to deficient trophoblast invasion and defective spiral artery remodelling  
256 which were associated with marked alterations in uterine and radial arteries  
257 haemodynamic, and a significative increase in blood pressure.

258

259 The results of this study show that both isoforms of HO are expressed in the rat  
260 implantation sites during pregnancy. Specifically, we observed the highest levels of  
261 HO-1 and HO-2 at mid-pregnancy, coinciding with the onset of trophoblast invasion  
262 into the rat uterine decidua (17) and suggesting that HO may be involved in this  
263 process, and therefore in the maternal vascular remodelling induced by these cells. A  
264 similar gestational pattern of both HO isoforms expression was previously described in  
265 rat uterine and placental tissues (18). Although the days of gestation analyzed were  
266 different, these authors found that uterine and placental HO-1 and HO-2 protein, and  
267 ARNm levels reached a peak at about day 16 of pregnancy, coinciding also with early  
268 stages of uterine trophoblastic invasion (18). In the human placental bed, endovascular  
269 and interstitial cytotrophoblasts express HO-1 and HO-2 suggesting that the activity of  
270 both HO isoforms could contribute to the control of trophoblast invasion and placental  
271 function (5,19). In this regard, it has been reported that the inhibition of HO in isolated  
272 human placenta produced a significant constriction in the placental vasculature,  
273 implying that the HO-CO system may participate in the regulation of blood flow in this  
274 organ (5). However, the role of HO in the trophoblast-dependent remodelling of human  
275 spiral arteries are poorly understood. We evaluated endovascular trophoblast invasion  
276 and vascular transformation in the mesometrial triangle of pregnant rats treated with the  
277 HO inhibitor, SnMP. Similar to humans, pregnant rats have a haemochorial placenta,  
with a deep intrauterine trophoblast invasion and a trophoblast-dependent spiral artery

278 remodelling (17,20). In the rat, trophoblasts penetrate into the uterine decidua between  
279 day 14 and 15 of pregnancy and extend into the myometrium as gestation advances  
280 (17). Vascular invasion of the mesometrial triangle is maximal at 18 days of gestation  
281 and is associated with loss of smooth muscle layer in the invaded vessels (17). We  
282 administered the HO inhibitor at day 14 of gestation, coinciding with the onset of  
283 trophoblast invasion, and we evaluated the remodelling of spiral arteries induced by  
284 these cells in the mesometrial triangle at day 19 of gestation. Vascular transformation of  
285 uterine arteries was reduced in pregnant rats treated with the HO inhibitor compared  
286 with normal pregnant animals. At day 19 of gestation, uterine arteries of rats with  
287 reduced placental HO activity showed a lower proportion of arterial lumen contours  
288 covered by trophoblast and more vascular smooth muscle than contours of the same  
289 vessels in normal pregnant rats, suggesting that HO enzyme contributes to structural  
290 changes in the uterine mesometrial vasculature. A greater proportion of vascular smooth  
291 muscle in the spiral arteries of rats with reduced HO activity may result in higher  
292 resistance to blood flow in these vessels and subsequently a deficient blood supply to  
293 the placenta and the fetuses. This is the first study showing that HO-CO system is  
294 involved in trophoblast-induced spiral artery remodelling, during late gestation.  
295 Although the ratio of wall to lumen diameter of spiral arteries has been found increased  
296 in pregnant HO-1 deficient mice compared with control animals, these studies were  
297 done during early gestation and they do not include data quantifying trophoblast  
298 invasion (21). In the mouse, this process is also initiated at midgestation, but in contrast  
299 with the rat, the invasion is restricted to the uterine mesometrial decidua and has a lesser  
300 endovascular contribution (17,20). For that reason, despite deep trophoblast invasion in  
301 human pregnancy occurs earlier than in the rat, pregnant rat is considered a better  
302 experimental model than the mouse for studies of uterine remodelling during  
303 pregnancy.

304 Impaired remodelling of maternal spiral arteries in our study was associated with  
305 significant alterations in uterine haemodynamics, an elevated number ( $P<0.05$ ) of  
306 reabsorbed pups and higher levels of blood pressure at late gestation, suggesting that the  
307 increase in this parameter, induced by the reduction of HO activity in pregnant rats, may  
308 be a consequence of an increased resistance in the uterine vasculature and insufficient  
309 blood supply to the uteroplacental unit. In this regard, it has been shown that  
310 mechanical reduction in uterine perfusion pressure provokes hypertension in pregnant  
311 rats (22) and mice (23) but not in nonpregnant animals. Although in our study the

312 increase in blood pressure observed at late gestation in response to HO inhibition is not  
313 excessive, the results suggest a considerable impairment of vascular adaptation to  
314 gestation. This is supported by the data obtained from non treated pregnant rats showing  
315 values of MAP around 14 mm Hg lower than treated pregnant rats. Finally these results  
316 are also consistent with studies showing that alterations of uterine artery blood flow are  
317 present in women with gestational hypertension and preeclampsia (24).

318 Uterine haemodynamics in our study was analyzed by Doppler ultrasonography.  
319 Doppler velocities, PSV, EDV, Vm and VTI increased in the uterine and radial arteries  
320 toward the end of pregnancy in normal pregnant rats. However these parameters did not  
321 change in the uterine vessels of rats with decreased HO activity. A progressive increase  
322 in systolic and diastolic velocities through gestation has been found in uterine arteries of  
323 rats and mice (25) indicating a direct relationship between these parameters and the  
324 gradual enhancement of blood flow to the utero-placental unit that occurs during  
325 pregnancy. These findings are consistent with a recent study showing that ligation of  
326 uterine vessels in mice causes a significant decline in uterine artery systolic blood  
327 velocity measured by Doppler ultrasonography (25). In human pregnancy, it has been  
328 reported that PSV and EDV show a marked elevation since early pregnancy, which is  
329 strongly correlated with the duration of gestation, therefore indicating change of  
330 compliance and resistance in the uterine circulation from the first weeks of gestation  
331 (26). On the other hand, Vm in the uterine artery has been also correlated with the  
332 gestational age in pregnant woman, demonstrating that this parameter can be also a  
333 good indicator of uterine vascular perfusion (27). Taken together, these data would  
334 indicate that a diminished HO activity may lead to an inadequate uteroplacental blood  
335 flow and a suboptimal blood supply to the fetuses. Although the contribution of the HO  
336 system to the uteroplacental circulation adaptation to pregnancy is clear in our study, the  
337 mechanism underlying this effect is unknown. Similar to our results, several studies  
338 have shown that a defective trophoblast invasion is associated with uterine artery  
339 Doppler alterations (15,28-30). However, uterine and radial arteries do not show  
340 trophoblast invasion. Thus, there are evidences indicating that flow through spiral  
341 arteries is not the only determinant of the Doppler uterine arterial waveform in  
342 pregnancy (3). In this regard, uterine artery waveforms from abdominal pregnancies  
343 show similar changes during gestation as seen in intrauterine pregnancies, despite the  
344 absence of spiral arteries trophoblast invasion (31,32). Therefore, we hypothesized that  
345 HO may be involved in the structural and functional changes observed in uterine and

346 radial arteries during pregnancy. During gestation, these vessels undergo enlargement in  
347 calibre and axial growth, which are trophoblast independent and probably mediated by  
348 hypertrophy and hyperplasia of smooth muscle and endothelial cells (2). HO system  
349 could contribute to these structural changes through its actions regulating VEGF levels,  
350 given that this factor induces vasodilation, stimulates endothelial mitosis and it has been  
351 associated with hypervascularization and vascular enlargement (2). This hypothesis is  
352 supported by the study of George et al (13), which have demonstrated that the increase  
353 in blood pressure induced by the administration of SnMP during late gestation is  
354 associated with a significant reduction in VEGF, therefore suggesting that lower levels  
355 of this proangiogenic factor may be mediating altered uterine and radial arteries  
356 remodelling, and uterine vasoconstriction induced by HO activity inhibition. Consistent  
357 with these results, it has also reported that HO-1 induction attenuates the hypertension  
358 and the decreased levels of VEGF induced by placental ischemia, suggesting that  
359 vascular endothelial dysfunction secondary to decreased uterine perfusion pressure  
360 might be improved in response to an inductor of this HO isoform (33). Finally,  
361 diminished levels of CO in response to reduced HO activity may also contribute  
362 directly to the reduction in uterine blood flow observed in our study.

363 On the other hand, the decrease in uterine blood flow induced by the inhibition  
364 of the HO activity could be partially mediating the alterations in trophoblast dependent  
365 transformation of spiral arteries. In this regard, it has been suggested that  
366 preconditioning of the spiral arteries precedes trophoblast invasion (11), and it has been  
367 reported that some maternal vessels undergo morphological changes without interaction  
368 with these cells (34). Lyall et al (5) demonstrated that HO-2 expression was reduced in  
369 placental endothelial cells of pregnancy disorders as preeclampsia or fetal growth  
370 restriction, suggesting that a reduction in CO levels in these cells could alter spiral  
371 artery dilatation prior to trophoblast invasion. One possible explanation would be that a  
372 reduced uterine blood flow and the shear stress could influence negatively the  
373 interactions between endothelial and vascular smooth muscle cells in the spiral arteries  
374 remodelling process (34). Consistent with this hypothesis it has been reported that  
375 human pregnancies with a low resistance uterine artery flow pattern obtained by  
376 Doppler ultrasound are associated with a more extensive trophoblastic invasion of the  
377 decidual vessels than pregnancies with a high resistance flow pattern (28).

378 In summary, the data obtained in this study indicate that HO-CO system play an  
379 important role in the adaptation of the uteroplacental circulation and the blood pressure

380 regulation during late gestation. Although the mechanisms mediating these effects have  
381 not been fully elucidated in the present study, our results appear to indicate that both  
382 trophoblast dependent and independent processes are involved. We speculate that the  
383 inhibition of the HO activity during late gestation could induce a reduction in uterine  
384 and radial arteries blood flow which may be contributing partly to the altered spiral  
385 arteries remodelling dependent of the trophoblast cell invasion. We also hypothesized  
386 that an increased resistance in the uterine circulation, during the last stages of gestation,  
387 can be a possible cause of the hypertension secondary to the HO activity inhibition.  
388 Further studies are necessary to determine the contribution of HO-CO system to the  
389 structural changes occurring in uterine and radial arteries during late pregnancy, and the  
390 impact that an inadequate transformation of these vessels in response to gestation could  
391 have in pregnancy disorders including hypertension, preeclampsia, and growth  
392 restriction.

393

394

395

396

397

398

399

400

#### 401 **Acknowledgements**

402 This work was supported by the Subdirección General de Proyectos de Investigación of  
403 Ministerio de Economía y Competitividad, Spain (BFU2013-49098-R and PII6/01556)  
404 and Fundación Séneca-Agencia de Ciencia y Tecnología de la Región de Murcia en el  
405 marco del PCTIRM 2011-2014 (19422/PI/14).

406 We wish to thank Carlos Manuel Martínez for his hepful advice about images.

407

408

#### 409 **REFERENCES**

410

411 [1] Pijnenborg R, Vercruysse L, Hanssens M. The uterine spiral arteries in human  
412 pregnancy: facts and controversies. *Placenta* 2006; 27 (9-10):939-98.

413

414 [2] Osol G, Mandala M. Maternal uterine vascular remodelling during pregnancy.  
415 *Physiology* 2008; 24:58-71.

416

- 417 [3] Burton GJ, Woods AW, Jauniaux En Kingdom JCP. Rheological and Physiological  
418 Consequences of Conversion of the maternal spiral arteries for uteroplacental blood  
419 flow during human pregnancy. *Placenta* 2009; 30(6):473-82.  
420
- 421 [4] Brosens I, Pijnenborg R, Vercruyssen L, Romero R. The great obstetrical syndromes  
422 are associated with disorders of deep placentation. *Am J Obstet. Gynecol* 2010;  
423 204(3):193-201.  
424
- 425 [5] Lyall F, Barber A, Myatt L, Bulmer JN, Robson SC. Hemeoxygenase expression in  
426 human placenta bed implies a role in regulation of trophoblast invasion and placental  
427 function. *FASEB J* 2000; 14(1):208-19.  
428
- 429 [6] Kreiser D, Nguyen X, Wong R, Seidman D, Stevenson D, Quan S, Abraham N,  
430 Dennery PA. Heme oxygenase modulates fetal growth in the rat. *Laboratory*  
431 *Investigation* 2002; 82(6):687-92.  
432
- 433 [7] Zhao H, Wong RJ, Doyle TC, Nayak N, Vreman HJ, Contag CH, Stevenson D.  
434 Regulation of maternal and fetal hemodynamics by heme oxygenase in mice. *Biology of*  
435 *reproduction* 2008;78: 744-51.  
436
- 437 [8] Linzke N, Schumacher A, Woidacki K, Crot BA, Zenclussen AC. Carbon monoxide  
438 promotes proliferation of uterine natural killer cells and remodelling of spiral arteries in  
439 pregnant hypertensive heme oxygenase-1 mutant mice. *Hypertension* 2014;63;580-88.  
440
- 441 [9] Kreiser D, Kelly DK, Seidman S, Stevenson DK, Baum M, Dennery PA. Gestational  
442 pattern of heme oxygenase expression in the rat. *Pediatric Research* 2003;54(2):172-78.  
443
- 444 [10] Zhao H, Wong RJ, Kalish FS, Nayak NR, Stevenson DK. Effect of heme  
445 oxygenase-1 deficiency on placental development. *Placenta* 2010; 30(10):861-88.  
446
- 447 [11] Zenclussen AC, Lim E, Knoeller S, Knackstedt M, Hertwig K, Hagen E, Klapp  
448 BF, Arck PC. Heme oxygenases in pregnancy II: HO-2 is downregulated in human  
449 pathologies pregnancies. *Am J Reprod Immunol* 2003;50(1):66-76.  
450
- 451 [12] Zenclussen ML, Casalis PA, El-Mousleh T, Rebelo S, Langwisch S, Linzke N,  
452 Volk HD, Fest S, Soares MP, Zenclussen AC. Haem oxygenase-1 dictates intrauterine  
453 fetal survival in mice via carbon monoxide. *J Pathol* 2011;225(2):293-304.  
454
- 455 [13] George EM, Hosick PA, Stec DE, Granger JP. Heme Oxygenase inhibition  
456 increases blood pressure in pregnant rats. *Am J Hypertension* 2013;26(7):924-30.  
457
- 458 [14] Caluwaerts S, Vercruyssen L, Luyten C, Pijnenborg R. Endovascular trophoblast  
459 invasion and associated structural changes in uterine spiral arteries of the pregnant rat.  
460 *Placenta* 2005;26:574-584.  
461
- 462 [15] Geusens N, Verlohren S, Luyten C, Taube M, Hering L, Vercruyssen L, Hanssens  
463 M, Dudenhausen JW, Dechend R, Pijnenborg R. Endovascular trophoblast invasion,  
464 spiral artery remodelling and uteroplacental haemodynamics in a transgenic rat model  
465 of preeclampsia. *Placenta* 2008:1-10.  
466

- 467 [16] Verlohren S, Geusens N, Morton J, Verhaegen I, Hering L, Herse F, Dudenhausen  
468 JW, Muller DN, Luft FC, Cartwright JE, Davidge ST, Pijnenborg R, Dechend R.  
469 Inhibition of trophoblast-induced spiral artery remodelling reduces placental perfusion  
470 in rat pregnancy. *Hypertension* 2010;56:304-310.  
471
- 472 [17] Ain R, Canham LN, Soares MJ. Gestation stage-dependent intrauterine trophoblast  
473 cell invasion in the rat and mouse: novel endocrine phenotype and regulation.  
474 *Developmental Biology* 2003;260(1): 176-190.  
475
- 476 [18] Kreiser D, Kelly DK, Seidman DS, Stevenson DK, Baum M, Dennery PA.  
477 Gestational pattern of heme oxygenase expression in the rat. *Pediatric Research*  
478 2003;54(2): 172-8.  
479
- 480 [19] Barber A, Robson SC, Myatt L, Bulmer JN, Lyall F. Heme oxygenase expression  
481 in human placenta and placental bed: reduced expression of placenta endothelial HO-2  
482 in preeclampsia and fetal growth restriction. *FASEB Journal* 2000;15: 1158-68.  
483
- 484 [20] Carter AM, Enders AC, Jones CJ, Mess A, Pfarrer C, Pijnenborg R, Soma H.  
485 Comparative placentation and animal models: patterns of trophoblast invasion-a  
486 workshop report. *Placenta* 2006;27 Suppl A:S30-33.  
487
- 488 [21] Linzke N, Schumacher A, Woidacki K, Croy BA, Zenclussen AC. Carbon  
489 monoxide promotes proliferation of uterine natural killer cells and remodelling of spiral  
490 arteries in pregnant hypertensive heme-oxygenase-1 mutant mice. *Hypertension*  
491 2014;63:580-88.  
492
- 493 [22] Llinás MT, Alexander BT, Capparelli MF, Carroll MA, Granger JP. Cytochrome  
494 P-450 inhibition attenuates hypertension induced by reductions in uterine perfusion  
495 pressure in pregnant rats. *Hypertension* 2004;43(3):623-8.  
496
- 497 [23] Fushima T, Sekimoto A, Minato T, Ito T, Oe Y, Kisu K, Sato E, Funamoto K,  
498 hayase T, Kimura Y, Ito S, Sato H, Takahashi N. Reduced uterine perfusion pressure  
499 (RUPP) model of preeclampsia in mice. *PLoS One* 2016 11(5):e0155426.  
500
- 501 [24] Pijnenborg R, Vercruyssen L, Brosens I. Deep placentation. *Best Pract Res Clin*  
502 *Obstet Gynaecol* 2011;25:273-285.  
503
- 504 [25] Bibeau K, Sicotte B, Béland M, Gaboury L, Couture R, St-Louis J, Brochu M.  
505 Placental underperfusion in a rat model of intrauterine growth restriction induced by a  
506 reduced plasma volume expansion. *PLoS One* 2016 11(1):e0145882.  
507
- 508 [26] Abd El Aal DE, Künzel W. Blood flow velocity in the uterine and external iliac  
509 arteries before and after termination of pregnancy. *European Journal of Obstetrics and*  
510 *Gynecology and Reproductive Biology* 1993;11-16.  
511
- 512 [27] Bower S, Vyas S, Campbell S, Nicolaidis KH. Color Doppler imaging of the  
513 uterine artery in pregnancy: normal ranges of impedance to blood flow, mean velocity  
514 and volume of flow. *Ultrasound Obstet. Gynecol.* 1992;2:261-265.  
515

- 516 [28] Prefumo F, Sebire NJ, Thilaganathan B. Decreased endovascular trophoblast  
517 invasion in first trimester pregnancies with high-resistance uterine artery Doppler  
518 indices. *Human Reprod.* 2004;19:206-209.  
519
- 520 [29] Lyall F, Robson SC, Bulmer JN. Spiral artery remodelling and trophoblast invasion  
521 in preeclampsia and fetal growth restriction: relationship to clinical outcome.  
522 *Hypertension* 2013;62(6): 1046-54.  
523
- 524 [30] Craven CM, Morgan T, Ward K. Decidual spiral artery remodelling begins before  
525 cellular interaction with cytotrophoblasts. *Placenta* 2018; 19: 241-252.  
526
- 527 [31] Acacio GL. Uterine artery Doppler patterns in abdominal pregnancy. *Ultrasound*  
528 *Obste Gynecol.* 2002;20:194-196.  
529
- 530 [32] Collins SL, Grant D, Black RS, Vellayan M, Impey L. Abdominal pregnancy: a  
531 perfusion confusion? *Placenta* 2011;32:793-795.  
532
- 533 [33] George EM, Cockrell K, Aranay M, Csongradi E, Stec DE, Granger JP. Induction  
534 of Heme Oxygenase-1 attenuates placental-ischemia induced hypertension.  
535 *Hypertension* 2011;57(5): 941-948.  
536
- 537 [34] Whitley GSJ, Cartwright JE. Cellular and molecular regulation of spiral artery  
538 remodelling: lessons from the cardiovascular field. *Placenta* 2010; 31: 465-474.  
539  
540  
541  
542  
543

1 **Figure legends**

2  
3 Figure 1.-Expression of HO-2 and HO-1 at the implantation site through gestation. (A)  
4 Representative Western blot. C means control protein. (B) Quantification of protein  
5 expression using densitometry. Densitometric values are expressed relative to  $\beta$ -actin  
6 expression.  $\ast=p<0.05$  vs. day 8.

7  
8 Figure 2.- (A) Mean Arterial Pressure (MAP) in virgin (Vir.) and pregnant rats (Preg.)  
9 treated intraperitoneally with vehicle or stannous mesoporphyrin (SnMP). (B) HO  
10 activity at the implantation site in pregnant rats treated intraperitoneally with vehicle or  
11 SnMP.  $\ast=p<0.05$  vs. virgin control rats.  $\dagger=p<0.05$  vs. pregnant control rats.

12  
13 Figure 3.- Mesometrial triangle at day 19 of pregnancy of a control pregnant rat (A) and  
14 a pregnant rat treated with SnMP (B) stained for KRT. Arrows on A and B indicate the  
15 localization of the vessel magnified below. Parallel cross-sections of a spiral artery  
16 immunostained for KRT, ACTA and PAS from a pregnant control rat (C,E,G) and from  
17 a pregnant rat treated with SnMP (D,F,H).

18  
19 Figure 4.- (A) Doppler flow velocity waveforms obtained at day 19 of gestation in the  
20 uterine and radial arteries of a pregnant control rat (Control) and of a pregnant rat  
21 treated with stannous mesoporphyrin (SnMP). (B) Changes in the uterine artery peak  
22 systolic (PSV) and end diastolic velocity (EDV) from day 14 to day 19 of gestation in  
23 pregnant rats treated with vehicle or the HO inhibitor, SnMP. (C) Changes in the radial  
24 artery PSV and EDV from day 14 to day 19 of gestation in pregnant rats treated with  
25 vehicle or the HO inhibitor, SnMP.  $\ast=p<0.05$  vs. day 14 of gestation.

Table 1.-Mean velocity (Vm) and velocity time integral (VTI) obtained in uterine and radial arteries from control pregnant rats and pregnant rats treated with SnMP, at days 14 and 19 of gestation.\*=p<0.05 vs. day 14.†=p<0.05 vs. control pregnant rats.

	Uterine Artery				Radial Artery			
	Vm		VTI		Vm		VTI	
	Day 14	Day 19	Day 14	Day 19	Day 14	Day 19	Day 14	Day 19
Control	414±19	573±49*	64±5	86±8*	100±9	164±12*	17±2	26±2*
SnMP	479±21	487±20	73±4	70±1	108±10	112±8 †	17±1	17±1 †

Table 2.- Endovascular trophoblast (EF), fibrinoid (F) and vascular smooth muscle (VSM) in spiral arteries of the whole mesometrial triangle of control pregnant rats and pregnant rats treated with SnMP, expressed as % of the total spiral artery contour length.

	Control	SnMP
% ET	59 ± 5	21 ± 3*
% F	42 ± 7	22 ± 3*
% VSM	16 ± 5	33 ± 5*

\*=p<0.05 vs. control pregnant rats.

Figure 1

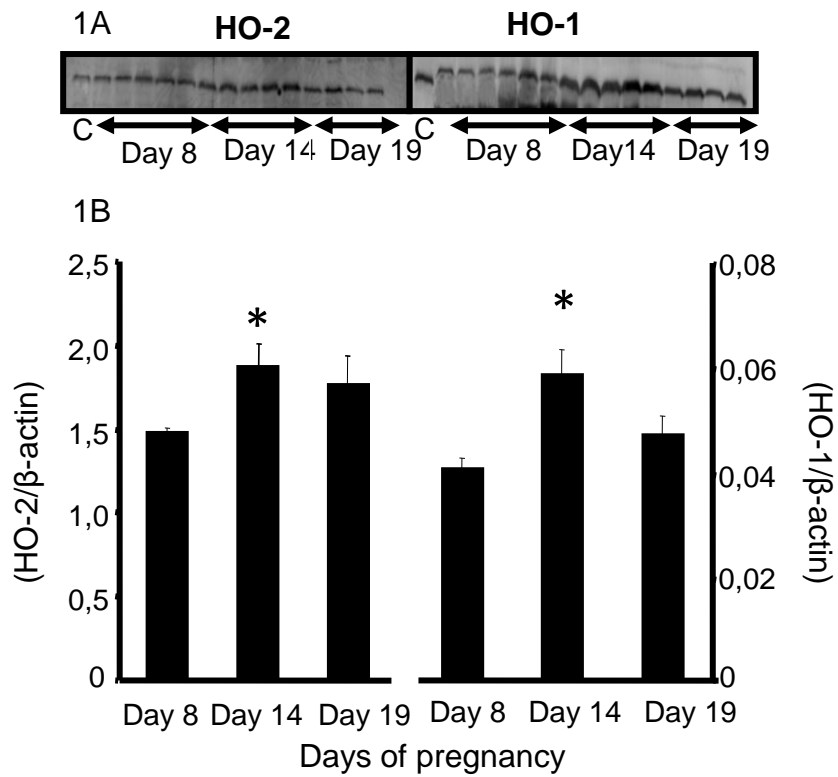
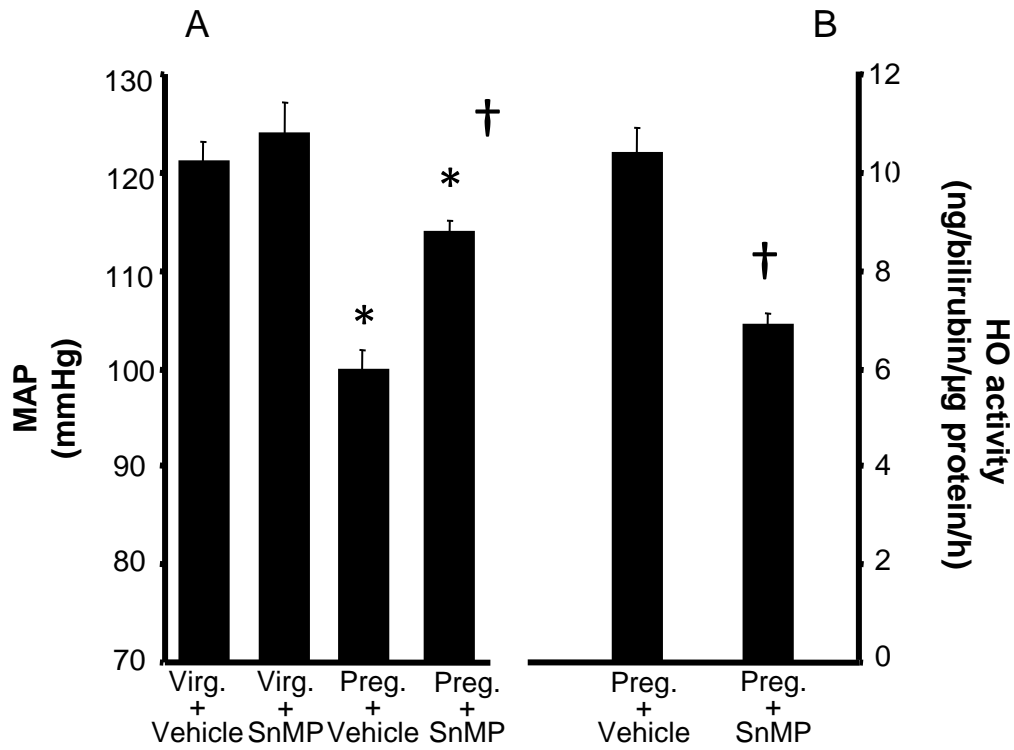


Figure 2



Figure

[Click here to download Figure: Figure3.pptx](#)

Figure 3

CONTROL

SnMP

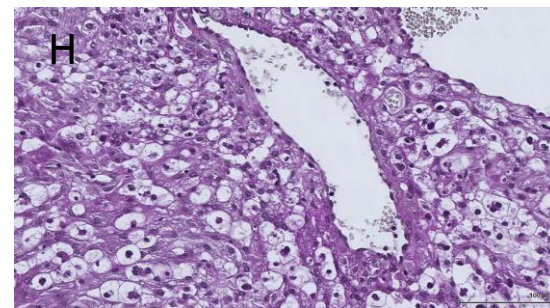
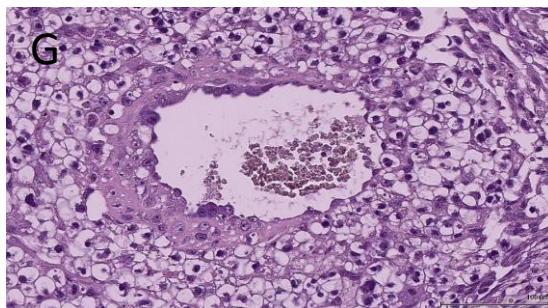
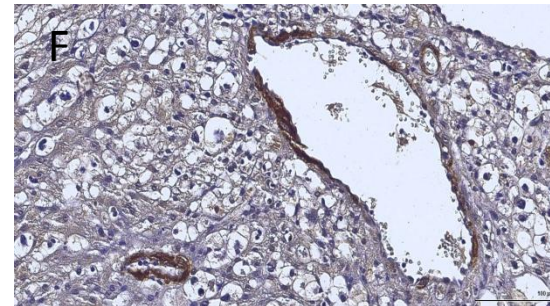
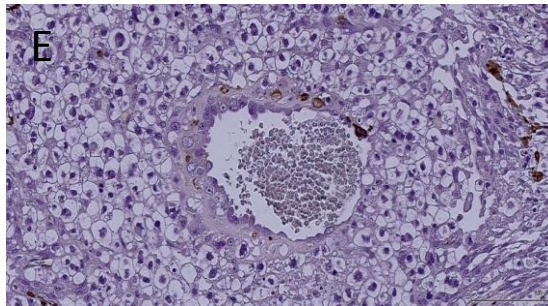
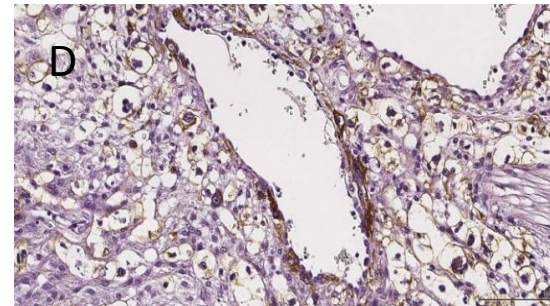
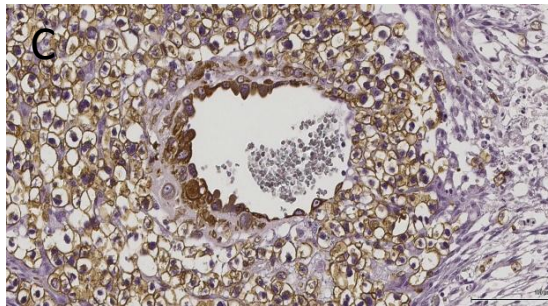
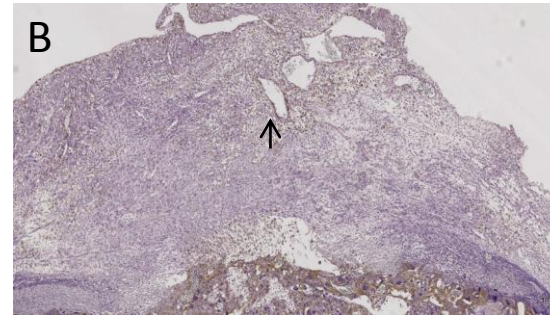
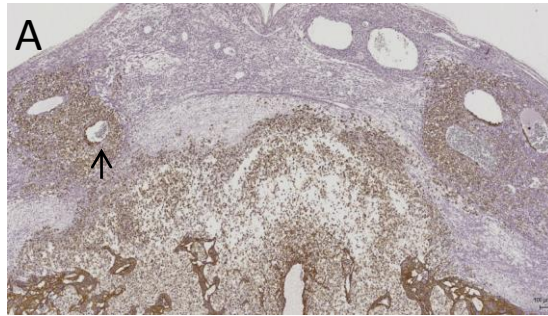
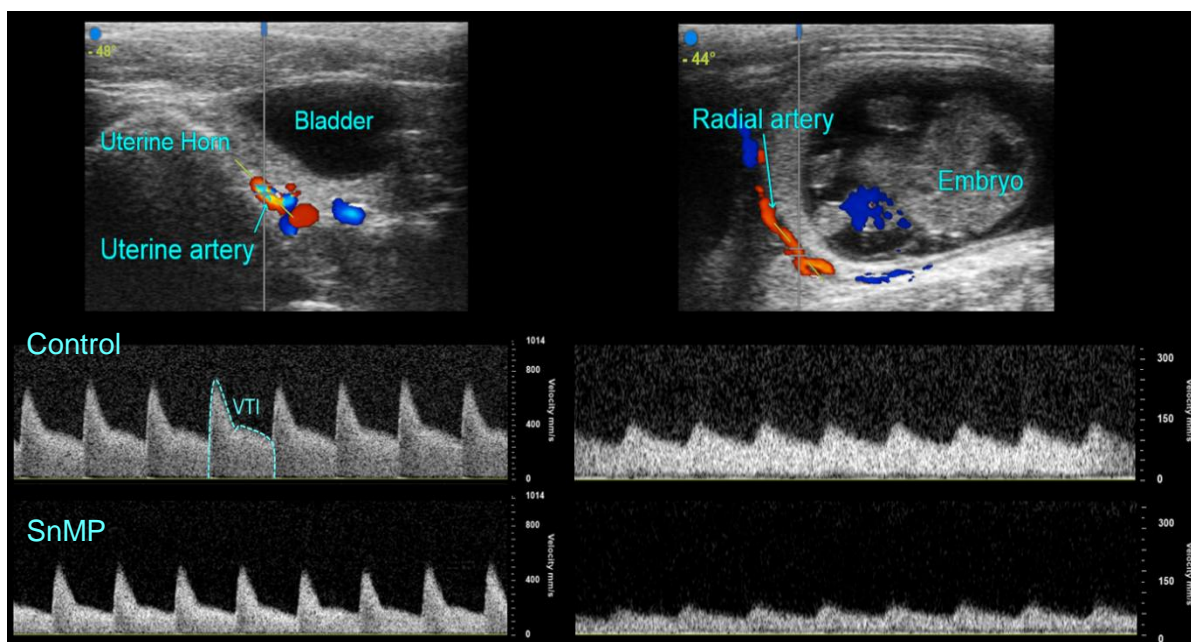
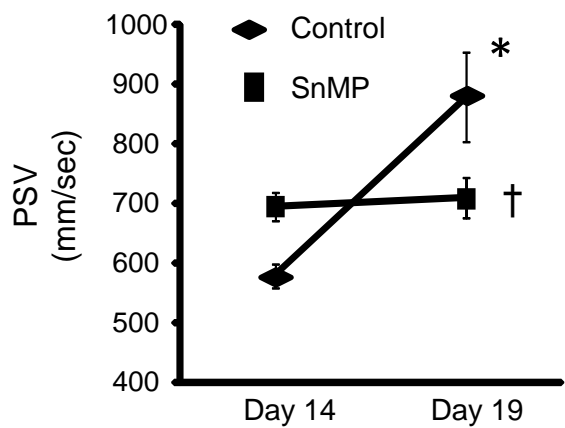


Figure 4

A



B Uterine artery



C Radial artery

